JOURNAL OF MATERIALS SCIENCE **35** (2000) 2881–2892

Predictive modelling of the properties and toughness of polymeric materials

Part III *Simultaneous prediction of micro- and macrostructural deformation of rubber-modified polymers*

R. J. M. SMIT*, W. A. M. BREKELMANS, H. E. H. MEIJER
Materials Technology (MaTe), Dutch Polymer Institute (DPI), Eindhoven University of Technology (TUE), P.O. Box 513, 5600 MB Eindhoven, The Netherlands
E-mail: Robert.Smit@unilever.com

The deformation behaviour of heterogeneous tensile bars is investigated by using the recently developed multi-level finite element method (MLFEM) that allows for a numerical coupling between the microscopic and macroscopic stress-strain behaviour, combined with an accurate elasto-viscoplastic constitutive model (single-mode compressible Leonov model) and a detailed finite element model of the microstructure. The method is used to predict the influence of the microstructure on localisation phenomena in plane strain notched and hour-glass-shaped polycarbonate and polystyrene tensile specimen with different volume fractions of non-adhering or adhering rubbery particles. In Part I and II of this series it was already suggested that elimination of the unstable post-yield strain softening behaviour of a polymeric material by appropriate microstructural modifications may be essential for toughening. The results of the multi-level analyses presented in this paper confirm this statement. It is shown that a stable post-yield response, resulting from microstructural adaptations, is indeed a prerequisite for the distribution of plastic strains over the whole macro- and microstructure: massive shearing is promoted by the introduction of voids in the polycarbonate or load bearing pre-cavitated rubbery particles in the polystyrene. Furthermore, it is shown that the voids indeed reduce the macroscopic dilative stresses to safe values. The results suggest that localisations of strain and stress will always occur on a macro and/or micro level. Catastrophic failure, however, can be postponed by stabilisation of the post-yield behaviour of the material and reduction of the macroscopic dilative stresses through appropriate microstructural adjustments.

1. Introduction

Toughness enhancement of polymeric systems has been and still is a major task in industrial laboratories of raw material manufacturers worldwide. Despite the many attempts to fundamentally understand the deformation and fracture behaviour of the generally heterogeneous polymeric systems involved, and despite the substantial progress nowadays realised in the modelling of important distinct and mostly isolated sub-processes in the microscopic and macroscopic mechanical behaviour of polymers, toughness enhancement in practice almost exclusively progresses along empirical routes. Many scientific (read: modelling) endeavours are, in fact, frustrated by the inability to predict the macroscopic mechanical behaviour, and thus toughness, of homogeneous or heterogeneous polymeric systems from their microstructural properties.

One typical element of continuous discussion is how tensile tests at moderate testing conditions relate to (notched) tensile toughness tests at high deformation rates. Often it is even stated that no relevant correlation exists between the two types of testing. Another, but similar, discussion concerns the basic question how the deformation on a micro-scale influences the macroscopic response. Since these questions are yet unsolved, progress in the improvement of mechanical properties of polymeric systems almost automatically implies the need for extensive experimental testing of newly developed systems on all the different length scales present. Consequently, the ultimate test for a new polymeric product is the classical 1 : 1 test (e.g. crash tests with bumpers in automotive applications). Such decisive tests are characterised by (i) simultaneous loading of micro- and macrostructure, and

* *Present Address*: Unilever Research Vlaardingen, P.O. Box 114, 3130 AC Vlaardingen, The Netherlands.

(ii) mutual interactions between local and global deformations. Apparently, from an experimental point of view, all the relevant micro- and macrostructural deformations must be taken into account simultaneously in order to obtain reliable results. This suggests that the incorporation of simultaneous micro-macro modelling is a prerequisite for a successful qualitative and quantitative prediction of the deformation behaviour of (heterogeneous) polymeric structures. The total absence of such a micro-macro approach in the literature may even be a possible explanation for the rather disappointing results of the fundamental research.

The aim of this paper is to provide a generally applicable methodology to elucidate and predict the deformation behaviour of heterogeneous polymeric systems by detailed finite element modelling, taking into account both macrostructure (e.g. a notched tensile bar) and microstructure (e.g. isolated rubber particles in a continuous glassy matrix). Part I of this series [1] considered the deformation and fracture behaviour of homogeneous amorphous polymer glasses, introducing the recently developed generalised compressible Leonov model, and explained the brittleness of polystyrene and toughness, but notch sensitivity, of polycarbonate by detailed finite element modelling of notched tensile bars with a minor defect. Furthermore, Smit *et al.* [2] introduced a homogenisation method that provides an unambiguously objective relationship between micro and macro deformations, entitled the multi-level finite element method (MLFEM), where a finite element model of the microstructure is used as a constitutive model in the macroscopic structure. Subsequently, two micromechanical studies [3, 4], focused on the definition of the (finite element) model of the microstructure, the so-called representative volume element (RVE), and investigated the effect of microstructural changes on the 'intrinsic' RVE averaged mechanical behaviour. The present paper combines the generalised Leonov model, the multi-level finite element method and the RVE concept to predict the mechanical behaviour of hour-glass shaped test specimens and notched tensile bars with voids or pre-cavitated rubber particles, in order to understand why and under what circumstances rubber modification has a positive influence on the deformation behaviour, especially on the toughness.

The paper starts with a brief introduction of the multi-level finite element method (MLFEM). Then, special, computationally advantageous, representative volume elements (RVEs) are introduced. Accordingly, a mutual comparison of the macroscopic strain localisations in hour-glass shaped tensile bars with three contrasting microstructures is performed, i.e. the slightly unstable homogeneous polycarbonate, the stable 30vol.% voided polycarbonate and the unstable 30 vol.% voided polystyrene. Subsequently, the effects of microstructural adaptations on the micro and macro deformations of notched tensile bars of PS or PC with voids or rubber particles are addressed, where the rubber is assumed to be pre-cavitated in order to avoid the necessity to model also the cavitation process inside the rubber. The paper ends with a discussion and conclusion where an attempt is made to qualify the polymeric systems as being brittle or tough by an estimation of their defect sensitivity and notch sensitivity.

2. Multi-level finite element method

The multi-level finite element method (MLFEM, see Reference [2]) is a novel homogenisation method that provides an accurate unambiguous relationship between the microscopic and macroscopic deformation and stresses. MLFEM enables a simultaneous prediction of both the macro deformations and micro deformations. The basis of the multi-level finite element approach is that in the integration points of the macroscopically meshed structure, for example a notched Izod test bar, the analysis descends to one level lower: the level of the RVE, the representative volume element. The RVE, which is in fact a finite element model of the heterogeneous microstructure which should be large enough to be representative, is used to decouple, in a computational sense, the macrostructure from the microstructure. The macro-micro relationship is obtained by the assumption that the local deformation and stress tensors in the macroscopic integration points are equal to the RVE averaged deformation and stress tensors. So, essentially, each individual RVE (with periodic boundary conditions which express that the RVE deforms as its direct neighbours) acts as a substitute constitutive model that provides the local macroscopic mechanical response. The connections between the RVEs in the different macroscopic integration points are, however, only made on the macro level. The macroscopic momentum balance equations combine the RVE deformations in such a way that equilibrium is macroscopically obtained. Hence, the multi-level finite element method provides the global response in the macroscopic structure through averaged stress/deformation fields, as well as the RVE responses through local stress/deformation fields, as exemplified in Fig. 1.

3. Prediction of the intrinsic mechanical behaviour of heterogeneous systems

In the present paper, the attention will be focused on the deformation behaviour of tensile bars of polystyrene and polycarbonate with 30 vol.% voids, and polystyrene with 30 vol.% perfectly adhering pre-cavitated rubber particles, similar to the systems introduced in Part II. The multi-level finite element method will be employed to predict the macro and micro deformations simultaneously. In order to obtain acceptable calculation times, however, the RVEs that provide the local macroscopic responses must be computationally inexpensive and numerically robust. The representative volume elements employed in the present analyses are, therefore, chosen to be point symmetric with a relatively simple geometry, as shown in Fig. 2 (compare with the RVEs shown in Fig. 12). The finite element meshes of the RVEs are composed of plane strain 8-node quadrilateral reduced integration elements and 6-node triangular elements. The constitutive behaviour of the matrix material is

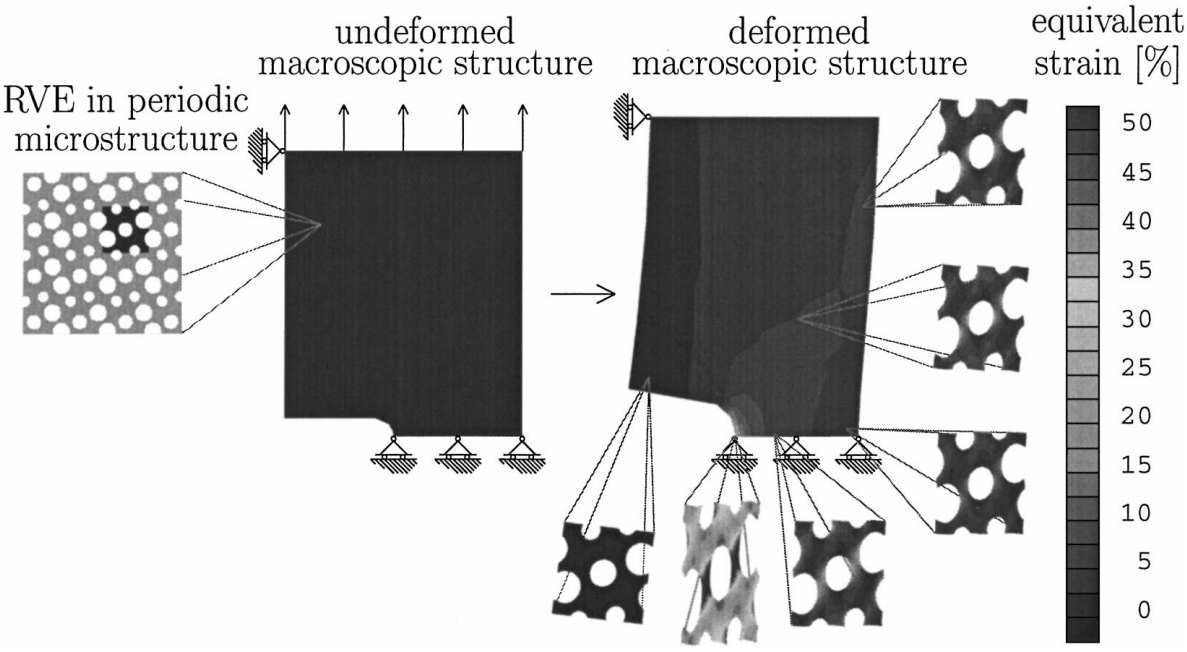

Figure 1 Example of a multi-level finite element analysis: deformation of a notched tensile bar of voided rubber with hypoelastic material behaviour. Notice the striking differences between macroscopic and local microscopic strains.

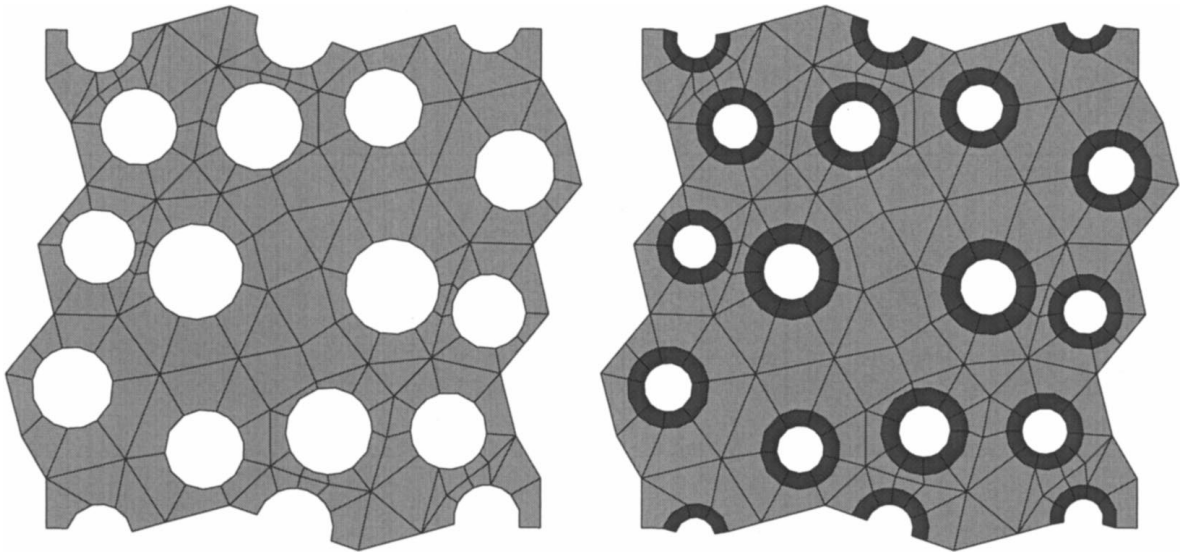

Figure 2 Plane strain models of RVEs used as constitutive models in the finite element simulation of the notched tensile bar, representing polystyrene or polycarbonate blended with 30 vol.% voids (left) or pre-cavitated rubber particles with a thick shell (right).

described by the generalised compressible single-mode Leonov model, introduced in Part I, and the behaviour of the rubber is predicted by a neo-Hookean model (see Part II), with a 30 MPa shear modulus and a 1000 MPa bulk modulus.

Fig. 3 displays the unidirectional responses of the coarse RVEs. Notice that the responses are qualitatively comparable to those of the more detailed RVEs shown in Figs 5 and 8 in Part II. For the evaluation of the strain fields in the subsequent sections, it is also important to remark that strains larger than 2% are, in fact, partially inelastic. This is a lower value than that for homogeneous PS or PC, where the transition occurs at approximately 3% strain.

Similar to the approach chosen in Part II, the problem of matrix crazing is not incorporated in this study. The averaged thickness of the ligaments between two inclusions is, therefore, assumed to be smaller than two craze fibril spacings (PC < 25 nm; PS: < 50 nm, see Kramer [5]).

4. Deformation behaviour of heterogeneous hour-glass shaped tensile bars

4.1. Problem definition

The importance of the microscopic mechanical response for the localisation of strains in plane strain hour-glass shaped tensile specimens has been investigated by single- and multi-level finite element simulations. Three distinct systems have been considered with characteristic post-yield responses: homogeneous polycarbonate (slightly unstable), 30 vol.%

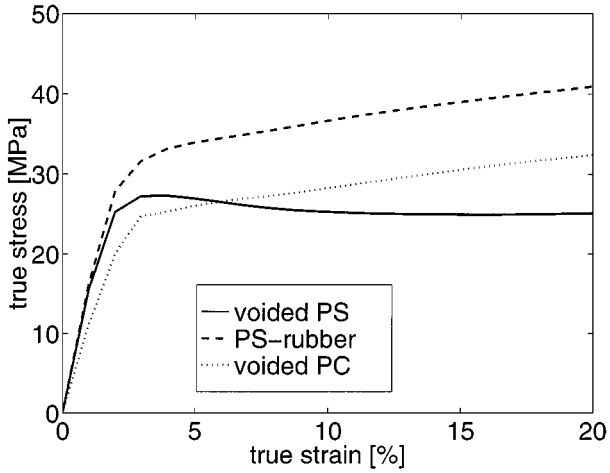

Figure 3 Predictions of the RVE averaged tensile stress versus true strain in plane strain extension (strain rate 0.01 s^{-1}).

voided polycarbonate (stable) and 30 vol.% voided polystyrene (unstable). The associated RVEs have been introduced in the previous section, the RVE averaged 'intrinsic' mechanical responses have been discussed in Part II. The geometry and the finite element model of the macroscopic specimen, composed of plane strain 8-node quadrilateral reduced integration elements, are shown in Figs 4 and 5, respectively. The specimen is chosen to be slightly asymmetric to obtain a preferred and thus controlled shear direction (the curved edges, with identical radii, are mutually shifted). In order to reduce calculation time, only one half of the point symmetric mesh is analysed. The macroscopic specimen is stretched with a constant strain rate of 0.001 s^{-1} up to a total nominal strain of 14%. Assuming that the particles are of the order of magnitude of 30 nm, the local temperature rise due to viscoplastic energy dissipation can be assumed to be negligible.

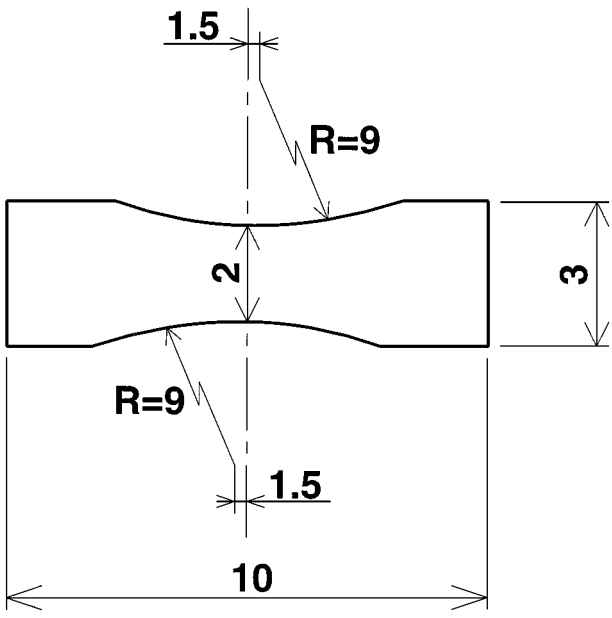

Figure 4 Dimensions of the undeformed plane strain hour-glass shaped tensile specimen.

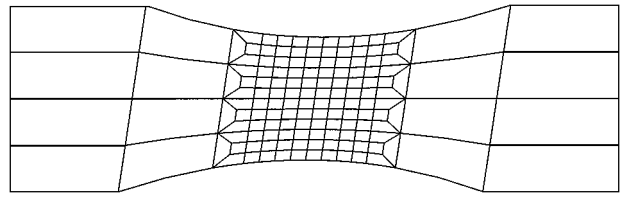

Figure 5 Finite element model of the undeformed plane strain hour-glass shaped tensile specimen. The dimensions are given in Fig. 4.

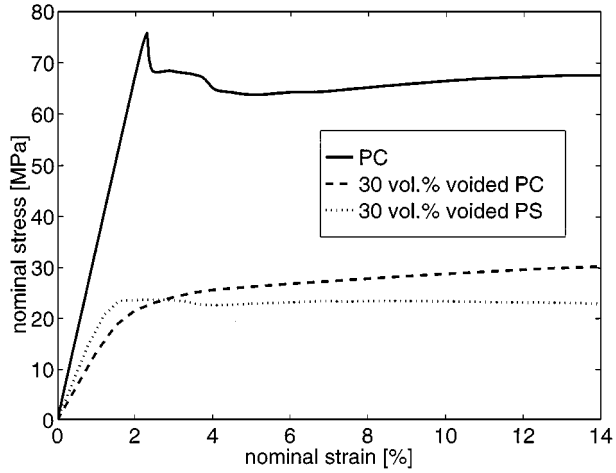

Figure 6 Nominal stress versus nominal strain of the macroscopic hour-glass shaped specimen, predicted for different microstructures and materials.

4.2. Homogeneous polycarbonate

The predicted macroscopic nominal stress response (defined with respect to the undeformed minimum cross sectional area of the specimen) is shown in Fig. 6. The equivalent† or principal strain, dilative stress and volume increase in the macroscopic samples at 4 and 14% nominal strain are plotted in Figs 7–9.

The homogeneous polycarbonate displays a typical, unstable, deformation behaviour. The deformation starts with an initial stiff overall elastic response. Then, between 2–2.5% nominal strain, a sudden load decrease is found caused by the first shear band formation (at an angle of 45° with the load direction). The shear band stabilises and grows between 2.5–3.5% strain. This is followed, between 3.5–4.5%, by a second load decrease, caused by the second shear band formation (at an angle of −45° with the load direction). Finally, between 4.5–14% strain, a neck is formed. Hence, the behaviour of the polycarbonate sample is characterised by a concentration of deformation in shear bands, neck formation and a large unstable post-yield stress drop (much 'apparent' softening). The contour plots of the dilative stress in Fig. 8 illustrate the triaxial nature of the stress state in the neck during neck formation. Notice that the critical craze-initiation stress of 90 MPa [1] is never reached. The maximum volume increase is small, approximately 3%, and therefore not visible in Fig. 9.

† The equivalent strain ε_{eq} is defined as the scalar norm of the logarithmic strain tensor $\boldsymbol{E}$, according to $\varepsilon_{eq} = \sqrt{\frac{2}{3}\boldsymbol{E}^d : \boldsymbol{E}^d}$.

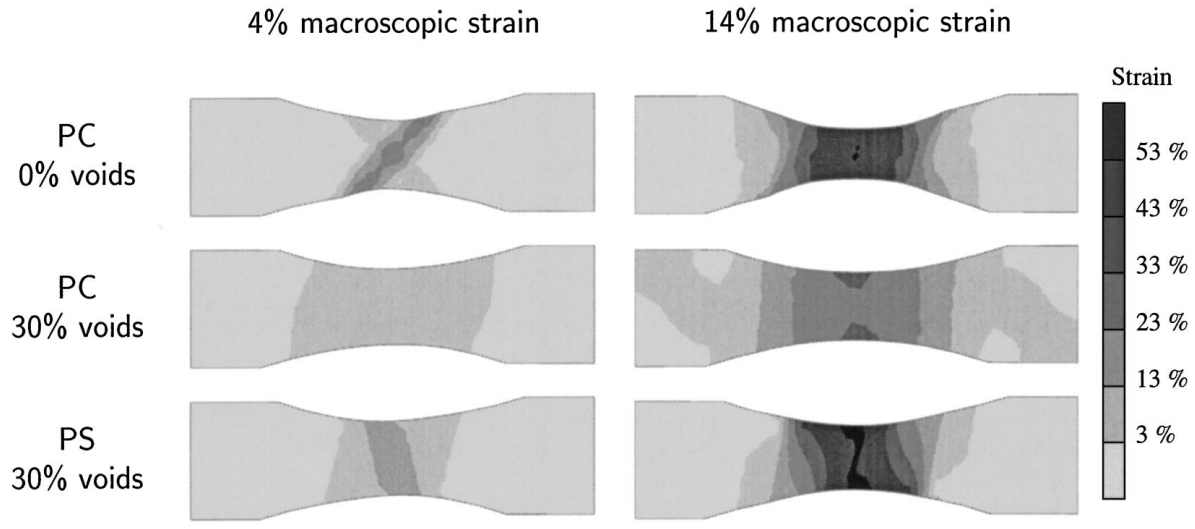

Figure 7 Contours of equivalent strain for the homogeneous PC and maximum principal logarithmic strain for the heterogeneous systems in the deformed hour-glass shaped tensile bar, predicted for different microstructures and materials.

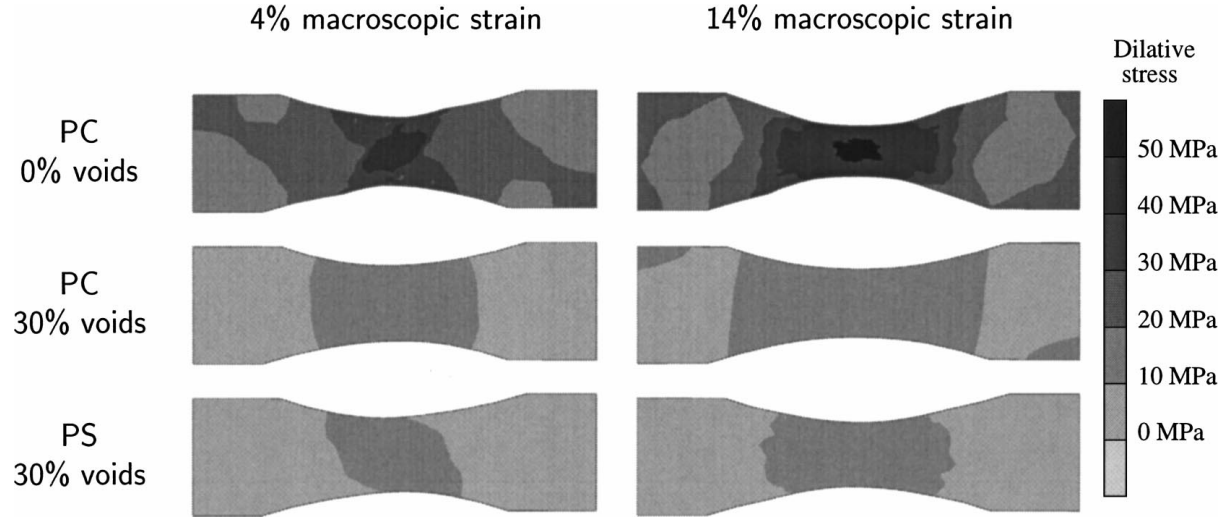

Figure 8 Contours of dilative stress in the deformed hour-glass shaped tensile bar, predicted for different microstructures and materials.

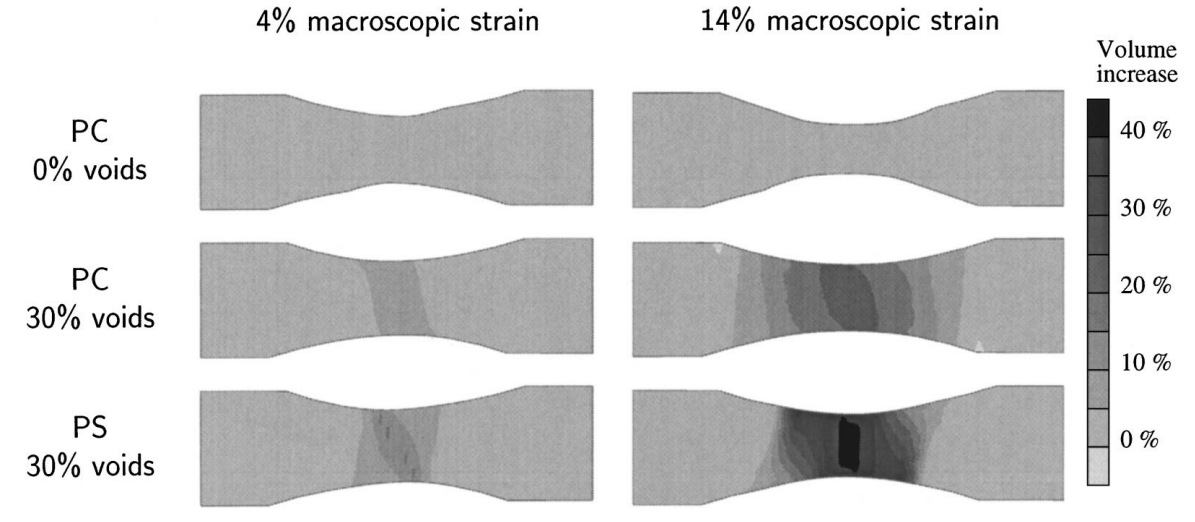

Figure 9 Contours of volume increase in the deformed hour-glass shaped tensile bar, predicted for different microstructures and materials.

4.3. Voided polycarbonate

The introduction of voids in polycarbonate results in a distribution of inelastic strains over the whole tensile bar, see Fig. 7: at 4% nominal strain, a broad shear band is formed perpendicular to the draw direction and at 14% strain nearly all the material deforms inelastically. No sharp shear band or neck is formed and the contraction of the bar is small compared to that of the homogeneous sample. The macroscopic volume in the hour-glass region increases strongly, indicating that the voids

grow in size. The contour plot of the dilative stress demonstrates that the growing voids also efficiently reduce the macroscopic dilative stress. The macroscopic stress-strain response, Fig. 6, shows that the rather homogeneous macroscopic deformation results in a smooth macroscopic stress-strain response, without any unstable load drops. The voids, of course, also reduce the yield stress and stiffness of the tensile bar.

4.4. Voided polystyrene

The results for the unstable voided polystyrene show a strong localisation of the deformation in a shear band perpendicular to the draw direction (see Figs 7 and 9). The volumetric strains are also concentrated in the shear band. The nominal stress-strain response, Fig. 6, indicates that the shear band formation is accompanied by a small macroscopic load decrease. The contour plot of the dilative stress, Fig. 8, shows that the voids also suppress the macroscopic dilative stress to safe values ($<$40 MPa, value adopted from Part I) in polystyrene, caused by and accompanied by a large local volume increase in the centre of the tensile bar.

4.5. Discussion

The results presented in this section clearly demonstrate that the macroscopic deformation behaviour of an hour-glass shaped tensile bar is indeed strongly affected by the averaged post-yield behaviour of the polymeric system. An unstable post-yield response consequently results in a strong localisation of macroscopic strains: in homogeneous PC sharp shear bands are formed at an angle of 45% with the load direction, while in voided PS a volumetric strain zone is formed perpendicular to the load direction. Stabilisation of the post-yield response by elimination of the macroscopic strain softening clearly prevents the formation of distinct deformation zones and promotes the spread out of plastic strains, as was shown for the 30 vol.% voided polycarbonate specimen.

Furthermore, it was shown that the introduction of microscopic voids also leads to an (expected) reduction of stiffness and yield stress of the macroscopic sample, while void growth results in a considerable macroscopic volume increase. The microstructural modifications were also responsible for a change of the orientation of the localisation zones: from homogeneous to 30 vol.% voided PC, the shear band angle changes from 45° to 90° with the load direction. A final but important consequence of the presence of the voids was a reduction of the macroscopic dilative stress, down to safe values.

In Part I it was already stated that the post-yield behaviour and especially the absence of strain softening is crucial for polymer toughening. The results of this section demonstrate that a stable macroscopic response promotes the enlargement of the inelastic deformation zone. Notice that such a deformation process is extremely beneficial for the energy absorption and thus the toughness of the specimen. The next section addresses the consequences of this toughening mechanism on the deformation behaviour of a notched tensile bar with a small imperfection at the notch tip.

5. Deformation behaviour of notched heterogeneous tensile bars

5.1. Problem definition

The toughness of different heterogeneous polystyrene and polycarbonate systems is investigated using the same strategy and test conditions as introduced in Part I: unidirectional extension (strain rate 0.001 s^{-1}) of plane strain notched test specimens with a minor defect, see Figs 10 and 11. The selection of an appropriate failure criterion for heterogeneous systems is, however, not clear yet and, therefore, the evolving stress and strain fields are mutually compared at different stages in the deformation process. For the multi-level finite element analyses, a coarser mesh has been generated in order to obtain acceptable calculation times (shorter than 2 weeks on a Silicon Graphics R8000 processor). Fig. 11 displays the mesh which is composed of plane strain 8-node quadrilateral reduced integration elements. Again, thermal effects are assumed to be negligible because of the low macroscopic strain rate and the small size of the heterogeneities. The MLFEM computations are carried on until excessive deformations inside the RVEs prohibit the continuation of the RVE calculations, because of severe mesh distortion.

The heterogeneous systems considered represent polystyrene or polycarbonate with 30 vol.% voids, or polystyrene with perfectly adhering voided rubber particles with a thick shell and a considerable modulus (30 MPa), similar to the ones described in Part II. The corresponding RVEs have been introduced in Section 3.

The local deformations of the heterogeneous microstructure with the severest load history, located at the root of the notch tip just below the centre of the defect, are analysed afterwards. During a post-processing step, the load history of the associated RVE (defined by an evolving deformation gradient tensor in time) is recovered from the macroscopic deformations. This load

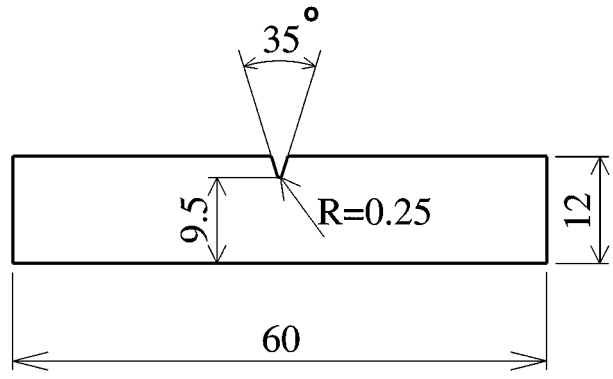

Figure 10 Dimensions (in mm) of the global geometry of the notched tensile test specimen.

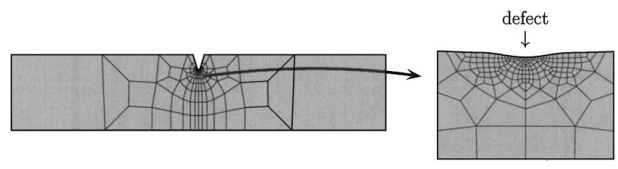

Figure 11 Plane strain finite element model of a notched tensile test specimen with a minor defect at the blunt notch tip. The geometric imperfection at the bottom of the notch tip is defined as a cosine shaped wave of length 0.04 R and amplitude 0.002 R.

history is subsequently prescribed to a more detailed RVE by imposing the evolving deformation gradient tensor to the RVE [2]. This procedure is only valid if the average mechanical response of the detailed RVE is comparable with the relatively coarse RVE used for the multi-level calculations. The RVEs used for the recovery of the micro deformations are shown in Fig. 12.

5.2. Voided polystyrene versus voided polycarbonate

The macroscopic nominal stress-strain curve, and the maximum macroscopic principal (logarithmic) strain and dilative stress in the notched tensile bar predicted for voided polystyrene and polycarbonate are shown in Figs 13–15, respectively. Again, the voids reduce the stiffness of the macroscopic specimens, and also reduce the dilative stress level down to safe values for both PS and PC. In the voided polystyrene, however, the unstable post-yield response of the microstructure results in a progressive deterioration as can be deduced from the maximum principal strain, see Fig. 14.

The contour plot of the maximum principal strain in voided polystyrene, Fig. 16, shows that the strain development is a consequence of the formation of a strong strain localisation, perpendicular to the draw direction. At a nominal strain of 0.6% the maximum local macroscopic principal strain is already 65% (see also Fig. 14).

The predicted localisation behaviour for the stable voided polycarbonate is depicted in Fig. 17. Again, the defect results in a local strain localisation zone. The maximum strain, however, shows a more gradual growth and is accompanied by a distribution of inelastic strains over a large volume of the sample. A local

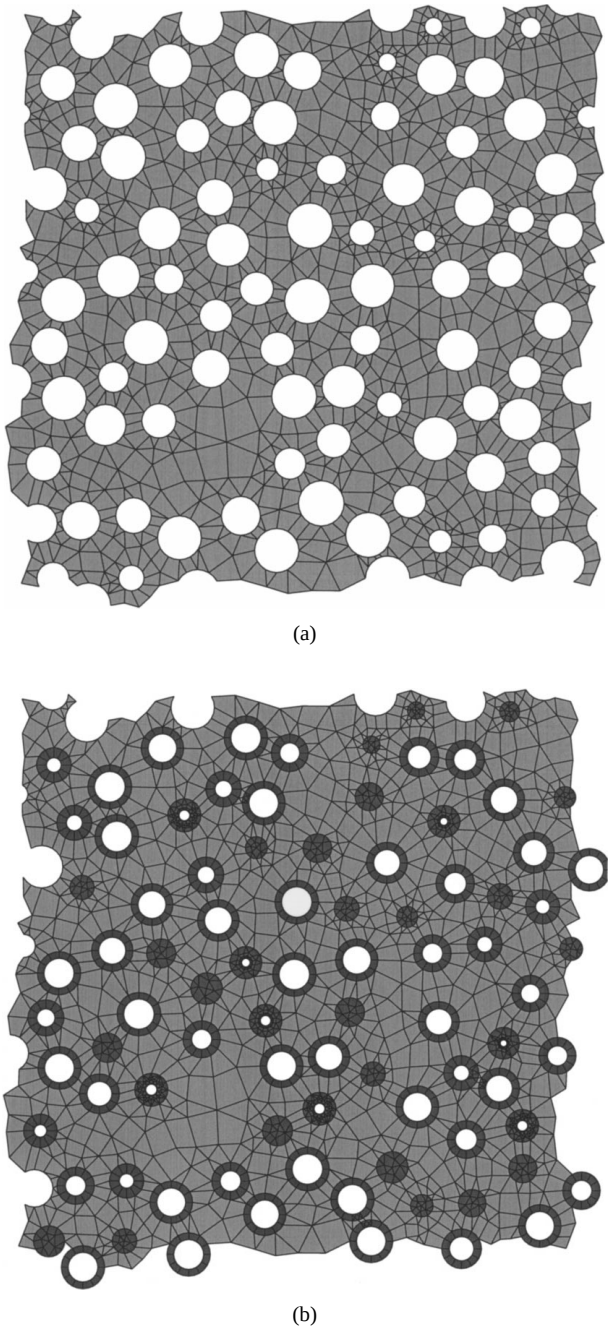

Figure 12 Geometry and finite element mesh of the detailed plane strain RVEs that are used for the recovery of the microstructural deformations at the root of the notch tip, representing a continuous matrix blended with (a) 30 vol.% voids or (b) 30 vol.% pre-cavitated rubber particles with a thick shell.

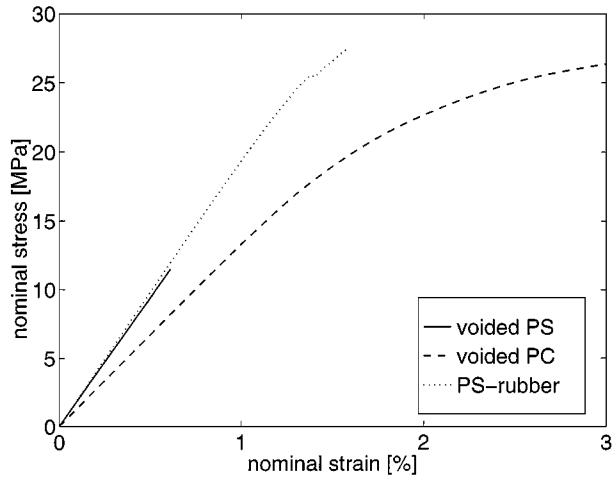

Figure 13 Nominal stress (defined with respect to the undeformed minimum cross-sectional area behind the notch tip) versus nominal strain of the notched test specimen, predicted for different microstructures and materials.

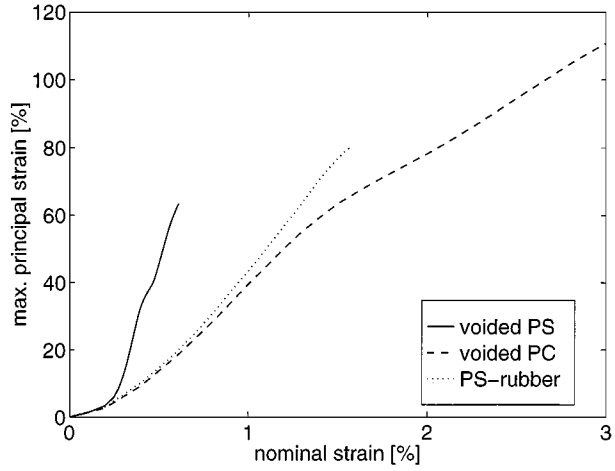

Figure 14 Maximum equivalent strain in the notched specimen as a function of nominal (macroscopic) strain, predicted for different microstructures and materials.

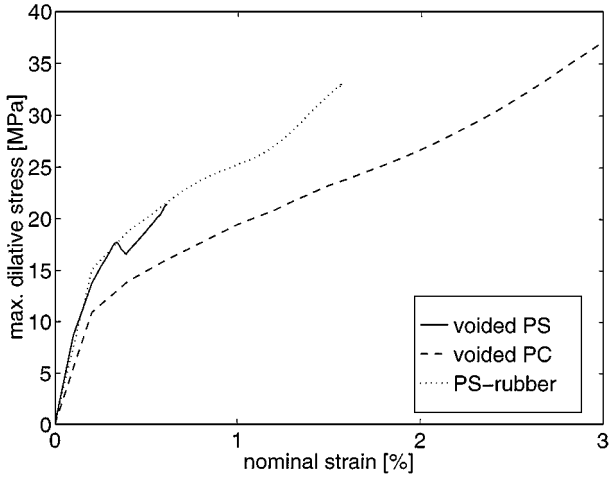

Figure 15 Maximum dilative stress in the notched specimen as a function of nominal (macroscopic) strain, predicted for different microstructures and materials.

macroscopic principal strain of 65% is reached at a nominal strain of 1.5%, which is considerably higher than the 0.6% for voided polystyrene. A comparison of the macroscopic strain fields of the 0.6% strained voided PS and the 1.5% strained voided PC emphasises the contrasting localisation behaviour: in voided polystyrene, a strong strain concentration is formed at the defect, while in voided polycarbonate, a large yield zone develops behind the notch tip.

Fig. 18 displays the reconstructed deformations of the severest loaded microstructures at the centre of the defect, just below the surface, at different (global) macroscopic strain levels. Again, the distinct post-yield mechanical responses of polystyrene and polycarbonate cause totally different microstructural deformations: polystyrene results in a concentration of deformation in dilatational bands, where the ligaments between the particles experience large deformations; polycarbonate results in a more diffuse type of deformation, where almost all the voids are incorporated in the deformation process. Apparently, an unstable type of material behaviour, like the one of voided PS, results in extreme localisations of strain in both macrostructure and microstructure. A stable type of behaviour, like that of voided PC, promotes the distribution of inelastic strains over a large domain of the material.

It is important to note that Fig. 18 illustrates, in fact, one striking micro-macro effect: small macroscopic strains (e.g. 0.4% for voided PS or 1% for voided PC) can be accompanied by large microscopic strains (>100% local strain in voided PS). Similar effects can be found in the crazing behaviour of homogeneous polystyrene, where macroscopic strains of 0.5–2% result in fibrilar draw ratio of 4 (140% logarithmic strain). The micro-macro effect is, however, the only major difference between the predicted microstructural deformations at the notch tip, and the unidirectional tensile tests on isolated RVEs that have been discussed in Part II. Those results confirm, therefore, that the deformation of the voided microstructure at the root of the notch tip is indeed comparable with the deformation of the

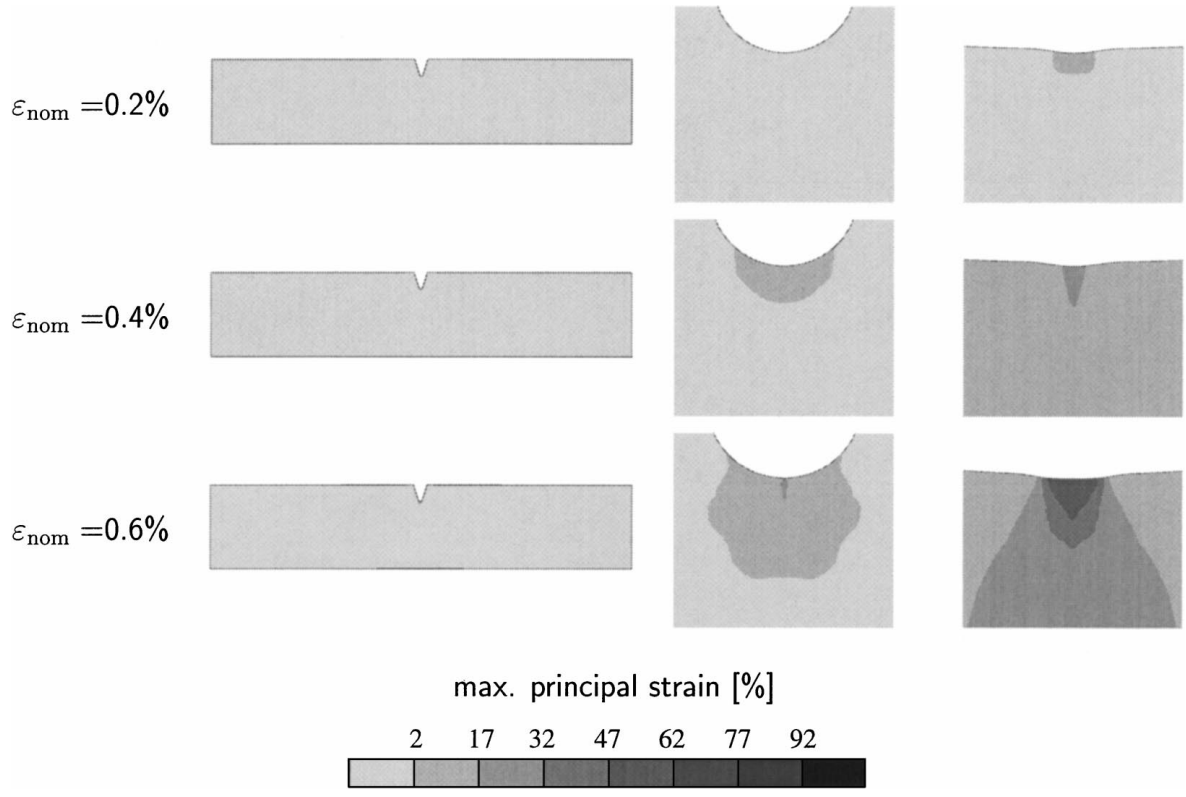

Figure 16 Contour plots of the maximum principal logarithmic strain in the total specimen (left), near the notch tip (middle) and defect (right), at different nominal strains, predicted for 30 vol.% voided polystyrene.

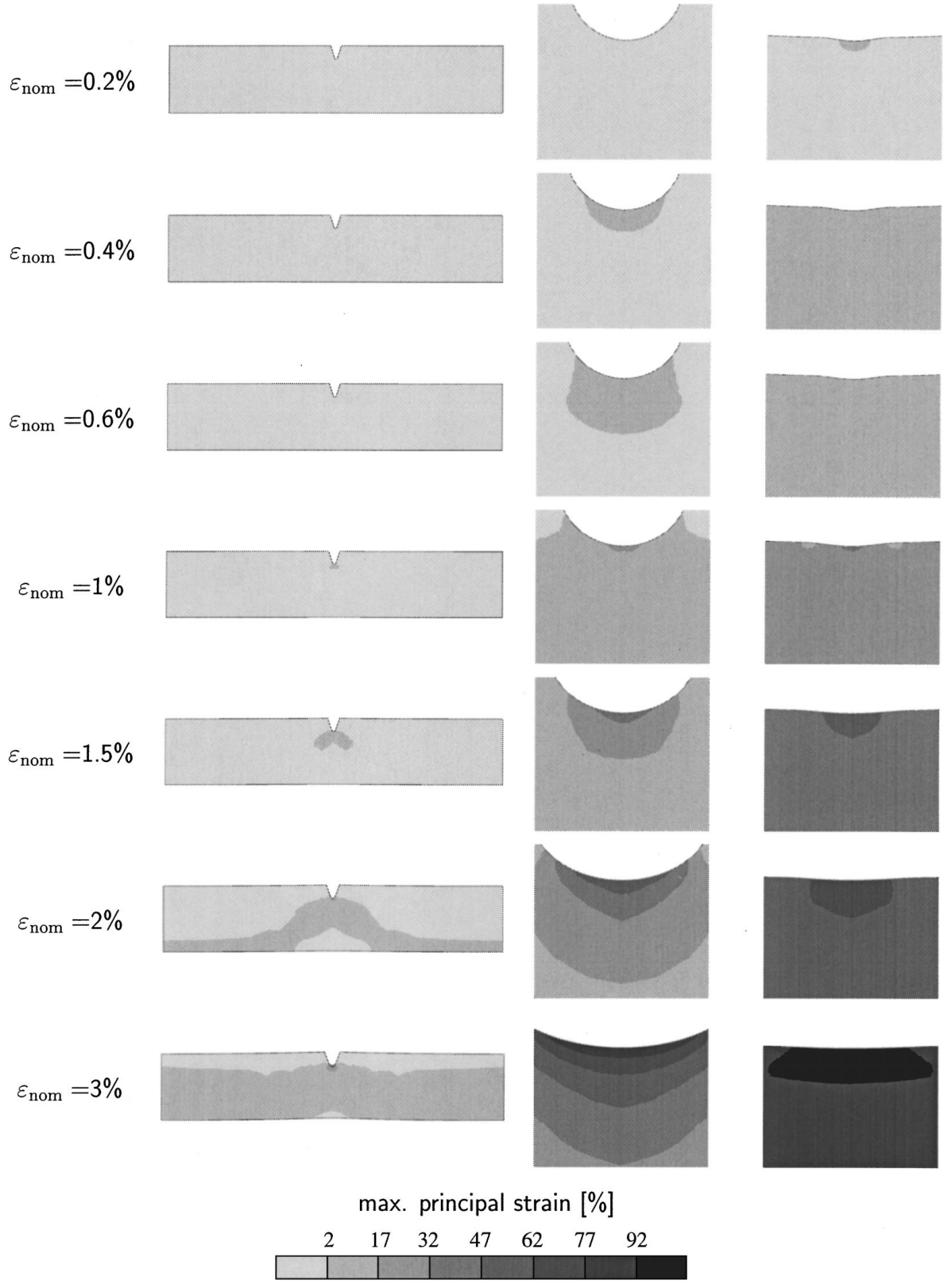

Figure 17 Contour plots of the maximum principal logarithmic strain in the total specimen (left), near the notch tip (middle) and defect (right), at different nominal strains, predicted for 30 vol.% voided polycarbonate.

same material in (higher-speed) uniaxial extension, as was suggested by Havriliak *et al.* [6]. Notice that this similarity is only valid if the failure behaviour can be expected to be concentrated at the surface of the notch tip. Thus, failure in the interior of the material, caused for instance by a critical dilative stress state (e.g. internal crazing in homogeneous PS or PC, see Part I), can not be examined and anticipated through (high-speed) uniaxial tensile tests. These conclusions at least partially answer the question posed in the introduction on the existence of a relation between tensile testing and notched toughness testing.

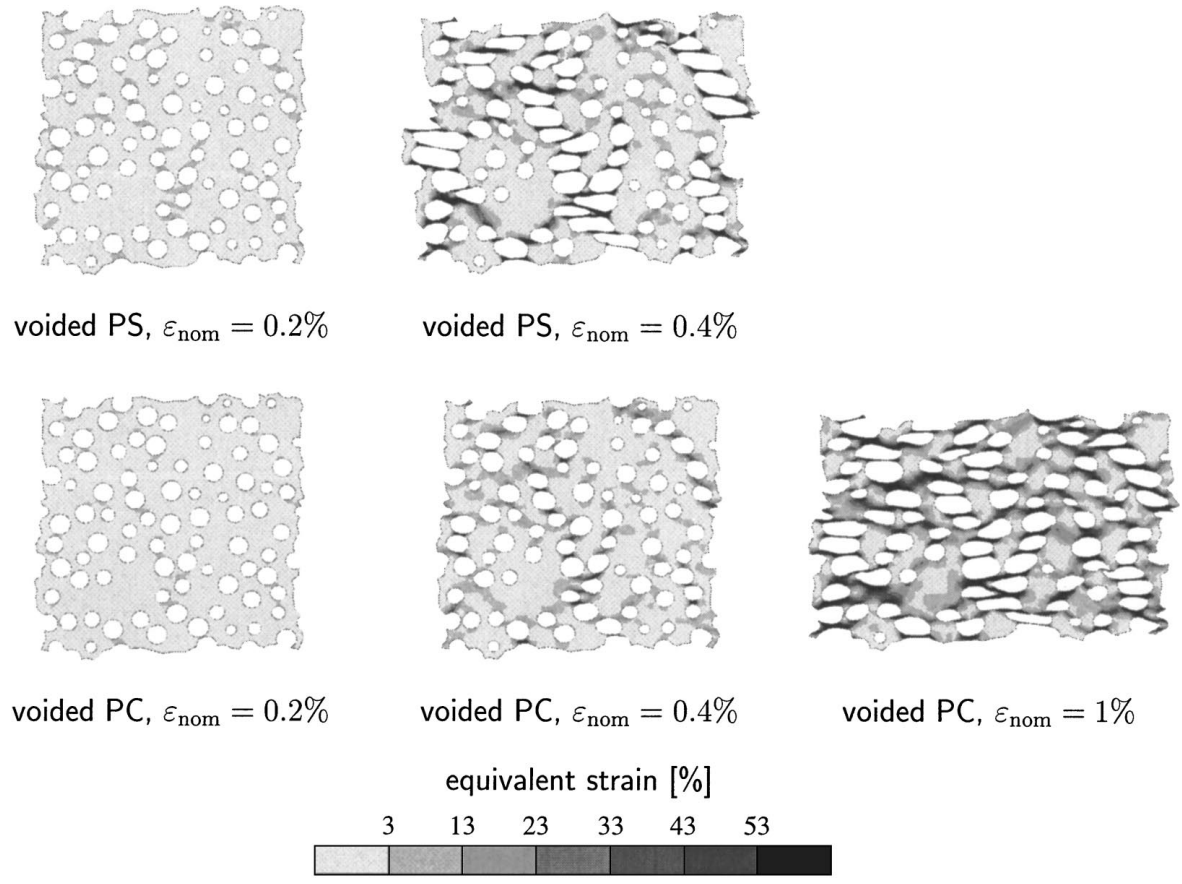

Figure 18 Contour plots of equivalent strain in the RVEs representing the deformed microstructure at the root of the notch tip at different macroscopic deformation stages, predicted for 30 vol.% voided polystyrene and polycarbonate.

The severe strain localisations shown in Figs 16 and 18 inevitably imply that unstable voided polystyrene is still extremely defect sensitive and thus brittle. The voided polycarbonate, on the contrary, displays a stable ductile behaviour because of the combination of a low defect sensitivity, a large inelastic strain zone behind the notch tip, and low macroscopic dilative stresses. So the toughness for notched polycarbonate tensile bars returns by the introduction of voids that reduce the macroscopic dilative stresses. The brittleness of (notched) polystyrene, however, remains unaffected by the addition of voids.

5.3. Effect of the properties of pre-cavitated rubber particles

The nominal stress-strain response and the maximum dilative stress and principal strain predicted for the notched polystyrene specimen with the thickshell system were already included in Figs 13–15. As expected, the macroscopic stiffness of the specimen is hardly affected by the introduction of the load-bearing pre-cavitated rubber particles with a shear modulus of only 30 MPa. The rubber particles have, however, a drastic influence on the maximum principal strain level. Compared to the results of voided polystyrene, the strain evolves more gradually and the evolution is, in fact, comparable to the strain evolution in voided polycarbonate. This is illustrated by the observation that a local maximum strain of 65% is reached at a macroscopic strain of 1.3%, which is large compared to the 0.6% nominal strain in voided polystyrene.

Fig. 19 shows contour plots of the maximum principal strain at different deformation stages. A comparison of Fig. 19 with the contour plots of voided polycarbonate (Fig. 17) clearly confirms the statement that the rubber filled polystyrene behaves similar to voided polycarbonate. The defect results in a strain localisation, but the strain concentration is also accompanied by a spread out of inelastic strains over a large volume of the sample. Because the voids sufficiently reduce the dilative stresses down to safe values (<40 MPa, see Fig. 15; the critical craze-initiation stress (40–50 MPa) for polystyrene has been adopted from Part I), a stable system is obtained with a reduced defect sensitivity and an eliminated notch sensitivity.

The reconstructed microstructural deformation at the centre of the defect, just below the surface of the specimen, is shown in Fig. 20. It is clearly visible that the core-shell rubber particles stabilise the deformation behaviour of the ligaments between the particles (compare Figs 20 and 18) and promote massive shearing of the polystyrene matrix. Hence, the addition of rubber particles results in a distribution of inelastic deformation over both microstructure and macrostructure.

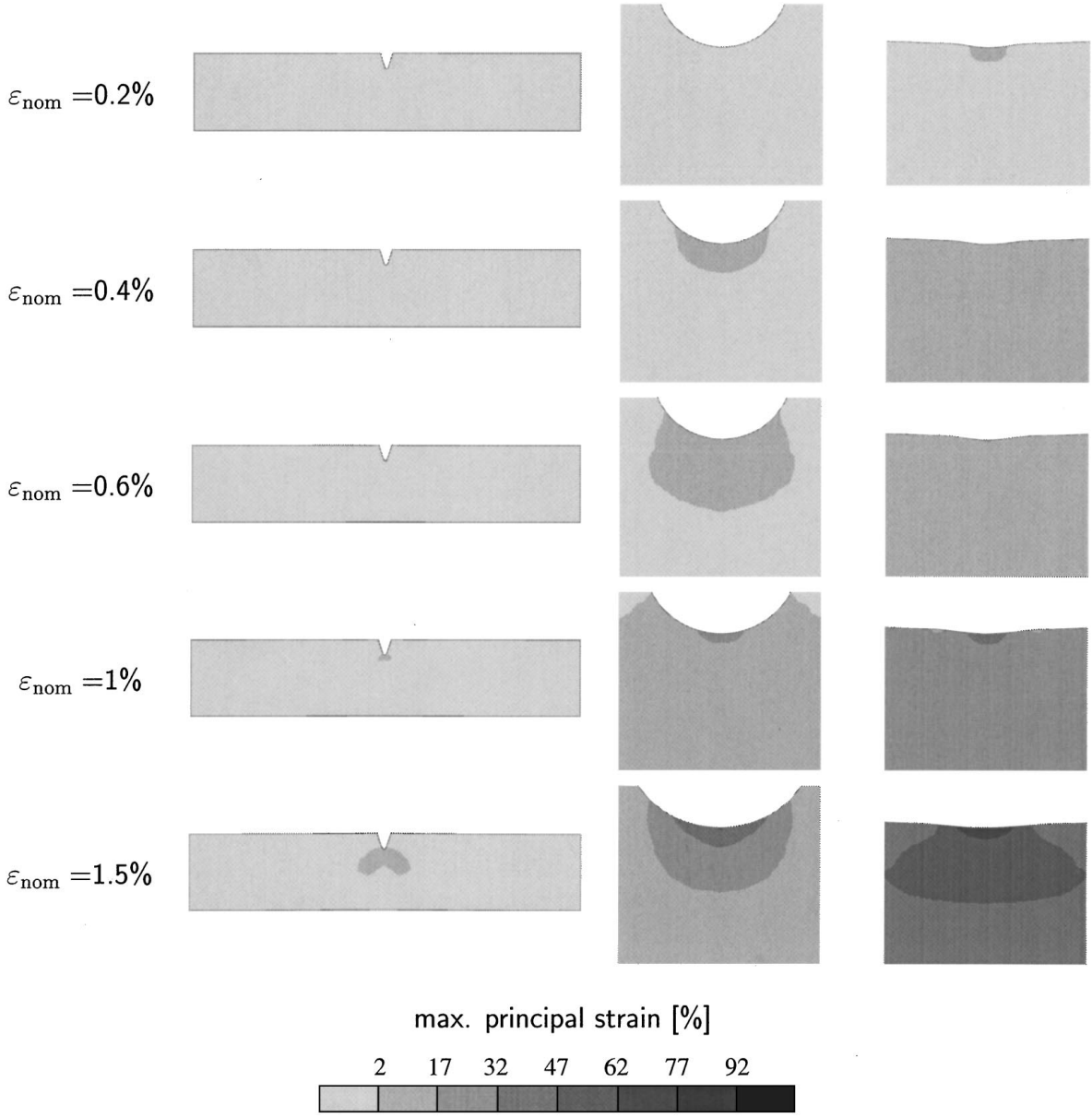

Figure 19 Contour plots of the maximum principal logarithmic strain in the total specimen (left), near the notch tip (middle) and defect (right), at different nominal strains, predicted for polystyrene with 30 vol.% pre-cavitated rubber particles.

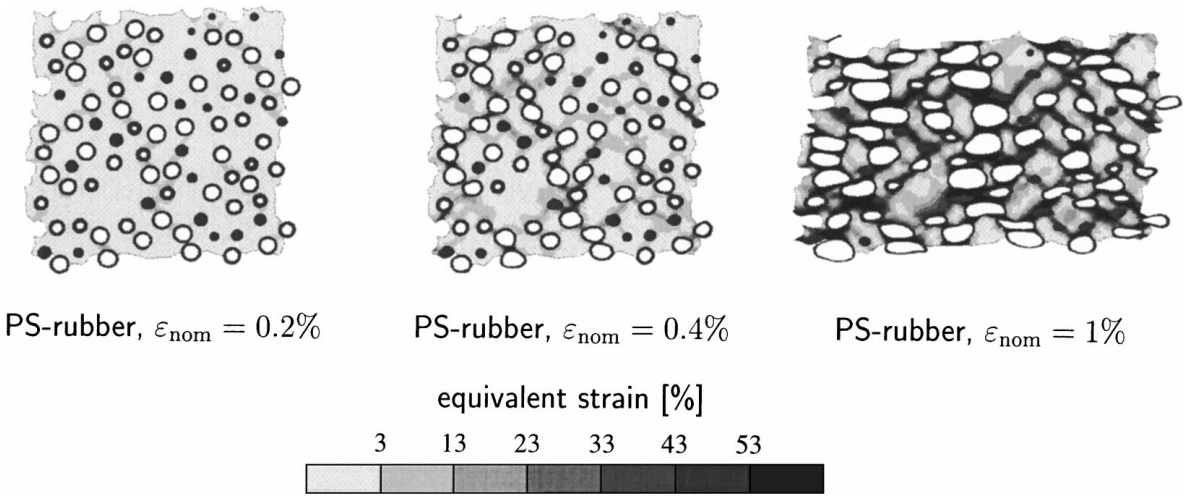

Figure 20 Contour plots of equivalent strain in the RVE representing the deformed microstructure at the root of the notch-tip at different macroscopic deformation stages, predicted for polystyrene with 30 vol.% pre-cavitated rubber particles.

6. Discussion and conclusions

The results of this paper and the findings of the foregoing homogeneous study (Part I) clearly demonstrate that stabilisation of the post-yield response of a heterogeneous system by appropriate microstructural modifications may indeed result in a more stable macroscopic behaviour. Going from unstable, via temporary unstable, to stable post-yield behaviour (by choosing subsequently homogeneous PS, voided PS, homogeneous PC, and voided PC), the macroscopic defect sensitivity disappears and the size of the localisation zone grows. As a result, more material is involved in the yield process and more energy is dissipated through plastic deformation. Those results suggest that this stabilisation mechanism is one of the key-mechanisms responsible for rubber toughening.

The importance of the stability of the post-yield response for the macroscopic behaviour is also emphasised by the shape of the localisation zones in the notched tensile bar. Numerous intersecting shear bands are formed at the root of the notch tip for temporary unstable homogeneous polycarbonate, while large yield zones at an angle of 45° with the load direction are formed behind the notch tip for stable voided polycarbonate. For unstable voided polystyrene, a strong, small and unstable deformation zone perpendicular to the load direction is developing at the defect. Apparently, the creation of voids should be accompanied by the stabilisation of the averaged post-yield response in order to prevent strong catastrophic strain localisations in the macrostructure. This statement is confirmed by the results of the stable (notched) polystyrene with load-bearing pre-cavitated rubber particles, where the defect sensitivity (and thus brittleness) was reduced and the deformation behaviour appeared to be similar to that of the voided polycarbonate.

The results of the simulations of the deforming microstructures demonstrate the necessity of the simultaneous micro-macro approach, since small macroscopic strains can result in large microscopic deformations. Furthermore, the reconstructed RVE deformations illustrate the obvious fact that the spread out of inelastic strains over the macrostructure must always be accompanied by a similar distribution of inelastic strains over the microstructure. Note that this supports the statement that a stable macrostructural deformation is a direct consequence of a stable microscopic deformation behaviour. The key-role of pre-existing voids or easily cavitating particles is also evident, since the voids effectively reduce the macroscopic dilative stresses. However, it was also shown in Fig. 18 that a low macroscopic strain could correspond to high local microscopic strains. This implies that early catastrophic failure of such heterogeneous polymeric systems could be caused by, for example, the excessive stretching of the ligaments between the particles. Unfortunately, a method to predict failure of a heterogeneous polymeric material is not available yet. However, based on the promising results of the reconstruction of the deformations of the microstructure (RVE), it is expected that a similar post-processing step combined with an appropriate failure model[‡] and the approach adopted in Part I (instantaneous macroscopic failure after reaching a certain critical stress or strain) may provide a reliable prediction of the catastrophic failure of the macrostructure.

Acknowledgements

We gratefully acknowledge the financial support of this work by the Dutch Technology Foundation (STW) (Grant EWT.3766).

References

1. R. J. M. SMIT, W. A. M. BREKELMANS and H. E. H. MEIJER, *J. Mater. Sci.* **35** (2000) 2855.
2. *Idem., Comput. Methods Appl. Mech. Engrg.* **155** (1998) 181.
3. *Idem., J. Mech. Phys. Solids* **47** (1999) 201.
4. *Idem., J. Mater. Sci.* **35** (2000) 2869.
5. E. J. KRAMER, in "Adv. in Polymer Sci., Vol. 52/53, edited by H. H. Kausch (Springer-Verlag, Berlin, 1983) Ch. 1.
6. S. HAVRILIAK, C. A. CRUZ and S. E. SLAVIN, *Polym. Eng. Sci.* **36** (1996) 2327.
7. M. H. WAGNER and J. SCHAEFFER, *J. Rheol.* **36** (1992) 1.
8. D. BROKKEN, W. A. M. BREKELMANS and F. P. T. BAAIJENS, *J. Mater. Proc. Techn.* **83** (1998) 192.

Received 25 August 1998
and accepted 19 November 1999

‡ E.g. so-called 'mechanical-melting', a collapse of the entanglement network by disentanglement (see, for example, Wagner and Schaeffer [7]), or discrete crack growth in the microstructure, similar to the work of Brokken *et al.* [8].